PROTEINS: Structure, Function, and Bioinformatics 54:58–70 (2004)

Docking Studies and Model Development of Tea Polyphenol Proteasome Inhibitors: Applications to Rational Drug Design

David M. Smith,[1] Kenyon G. Daniel,[1] Zhigang Wang,[2] Wayne C. Guida,[1,3] Tak-Hang Chan,[2] and Q. Ping Dou[1]*

[1]*Drug Discovery Program, H. Lee Moffitt Cancer Center and Research Institute, and Departments of Biochemistry and Molecular Biology and Interdisciplinary Oncology, College of Medicine, University of South Florida, Tampa, Florida*
[2]*Department of Chemistry, McGill University, Montreal, Quebec, Canada*
[3]*Department of Chemistry, Eckerd College, St. Petersburg, Florida*

ABSTRACT **Previously, we demonstrated that natural and synthetic ester bond-containing green tea polyphenols were potent and specific non-peptide proteasome inhibitors. However, the molecular mechanism of inhibition is currently unknown. Here, we report that inhibition of the chymotrypsin activity of the 20S proteasome by (−)-epigallocatechin-3-gallate (EGCG) is time-dependent and irreversible, implicating acylation of the β5-subunit's catalytic N-terminal threonine (Thr 1). This knowledge is used, along with in silico docking experiments, to aid in the understanding of binding and inhibition. On the basis of these docking experiments, we propose that (−)-EGCG binds the chymotrypsin site in an orientation and conformation that is suitable for a nucleophilic attack by Thr 1. Consistently, the distance from the electrophilic carbonyl carbon of (−)-EGCG to the hydroxyl group of Thr 1 was measured as 3.18 Å. Furthermore, the A ring of (−)-EGCG acts as a tyrosine mimic, binding to the hydrophobic S1 pocket of the β5-subunit. In the process, the (−)-EGCG scissile bond may become strained, which could lower the activation energy for attack by the hydroxyl group of Thr 1. This model is validated by comparison of predicted and actual activities of several EGCG analogs, either naturally occurring, previously synthesized, or rationally synthesized. Proteins 2004;54:58–70.**

Key words: 20S proteasome; β5-subunit; chymotrypsin-like activity; EGCG; green tea; organic synthesis; computation; drug discovery

INTRODUCTION

The proteasome is a massive multicatalytic protease complex that is responsible for degrading most of the cellular proteins.[1,2] The 20S-core particle of the 26S proteasome is barrel-shaped, and the sites of proteolytic activity reside on the interior. The eukaryotic proteasome contains three known activities, which are associated with its β-subunits. These are the chymotrypsin-like (cleavage after hydrophobic residues, β5-subunit), trypsin-like (cleavage after basic residues, β2-subunit), and caspase-like (cleavage after acidic residues, β1-subunit) activities.[3] These three activities depend on the presence of an N-terminal Thr (Thr 1) residue.[2] The hydroxyl group on the side chain of Thr 1 is responsible for catalyzing cleavage of peptides through nucleophilic attack (addition-elimination mechanism). Near this N-terminal threonine, binding pockets recognize the side-chains of peptides and give each catalytic site its specificity. The S1 pocket of the β5-subunit is defined by the hydrophobic residues, Ala 20, Val 31, Ile 35, Met 45, Ala 49, and Gln 53,[2] and this binding pocket has been shown to be important for substrate specificity and binding of several types of proteasome inhibitors.[4,5]

The ubiquitin/proteasome-dependent degradation pathway plays an essential role in up-regulation of cell proliferation, down-regulation of cell death, and development of drug resistance in human tumor cells, suggesting the use of proteasome inhibitors as potential novel anticancer drugs.[6,7] This hypothesis has been supported by results using various cell cultures, animal models, and clinical trials. In a broad range of cell culture models, proteasome inhibitors rapidly induce tumor cell apoptosis, selectively trigger programmed cell death in the oncogene-transformed, but not normal or untransformed cells, and are able to activate the death program in human cancer cells that are resistant to various anticancer agents.[6–9] Inhibition of the chymotrypsin-like, but not trypsin-like, activity has been found to be associated with induction of tumor cell apoptosis.[8,9] In different animal studies, proteasome inhibitors suppress tumor growth via induction of apoptosis and inhibition of angiogenesis.[10,11] MLN-341 (formerly PS-341) is a potent and selective dipeptidyl boronic acid

Grant sponsor: National Cancer Institute-National Institutes of Health; Grant sponsor: the United States Army Medical Research and Material Command; Grant sponsor: H. Lee Moffitt Cancer Center and Research Institute; Grant sponsor: Natural Science and Engineering Research Council of Canada; Grant sponsor: Molecular Imaging Core Facility at Moffitt Cancer Center and Research Institute.

*Correspondence to: Q. Ping Dou, Barbara Ann Karmanos Cancer Institute, and Department of Pathology, Wayne State University School of Medicine, 508 & 516 HWCRC, 110 E. Warren Ave., Detroit, MI 48201. E-mail: doup@karmanos.org

Received 19 December 2002; Accepted 15 May 2003

compound that inhibits the chymotrypsin-like activity of the 20S proteasome.[12] This proteasome inhibitor is currently being developed for the potential treatment of human hematological malignant neoplasms and solid tumors.[13,14] Preliminary data from phase I and II clinical trials confirm the antitumor activity of MLN-341, although some associated side effects were observed.[13,14] The mechanism by which MLN-341 inhibits the proteasome has not yet been determined by X-ray diffraction experiments. However, the proteasome-inhibition mechanism of another peptide inhibitor $LLnL^2$ and non-peptide inhibitors lactacystin[2] and the macrocyclic compound TMC-95[15] have been confirmed by X-ray diffraction. Understanding how these inhibitors function at the molecular level will give insight into the structural studies of other proteasome inhibitors where X-ray crystal structures are not available. These studies thereby show that the proteasome is an excellent target for developing pharmacological anticancer drugs.

Tea, the most popular beverage in the world, is consumed by more than two thirds of the world's population. Several epidemiological studies have provided evidence for the cancer-preventive properties of green tea.[16–19] Furthermore, animal studies have also suggested that green tea polyphenols could suppress the formation and growth of various tumors.[20–24] Although numerous cancer-related proteins are affected by tea polyphenols,[25–27] the molecular basis for tea-mediated cancer prevention remains unknown. We recently reported that the naturally occurring ester bond-containing green tea polyphenols (GTPs), such as (−)-epigallocatechin-3-gallate [(−)-EGCG, Fig. 1(A)], possess the ability to inhibit proteasome activity both in vitro and in vivo.[28] Moreover, we demonstrated that in a cellular extract, (−)-EGCG inhibits the β5-mediated chymotrypsin-like and β1-mediated caspase-like activities, but not β2-mediated trypsin-like activity, of the proteasome.[28] In addition, we discovered that synthetic GTPs with an ester bond, such as (+)-EGCG [Fig. 1(A)], were also able to potently and selectively inhibit the chymotrypsin-like activity of the proteasome.[29] It appears that a center of nucleophilic susceptibility resides at the ester bond-carbon in these polyphenols.[28,29] On the basis of these results, we proposed that this electrophilic carbonyl carbon might play a role in proteasomal inhibition by acylating Thr1 in the active site. This proposed mechanism of ester bond-based nucleophilic attack is similar to that of lactacystin-based inhibition.[4] However, until now, the precise mechanism of proteasome inhibition by GTPs has not been explored.

The purpose of the present study was to build a mechanistic model to describe how EGCG binds the proteasome before attack and cleavage of its ester bond.[28] Because the chemistry of ester bond cleavage would in all likelihood not allow for an EGCG-proteasome complex or subsequent tetrahedral intermediate to be captured by X-ray diffraction, another available tool for investigating the putative interaction between EGCG and the proteasome for rational drug design is computational docking. In the present study, for the first time, we demonstrate that (−)-EGCG is an irreversible mechanism-based inhibitor of the chymotrypsin-like activity of 20S proteasome. On the basis of this finding, we establish a docking model for how (−)-EGCG interacts with the β5-subunit of the 20S proteasome. This model is verified by application of several other natural and synthetic EGCG analogs, because their docking free energy could be used to predict their actual proteasome-inhibitory activity. Finally, the proteasome inhibition model of (−)-EGCG is further validated by rationally designing and synthesizing two EGCG-amide compounds, followed by comparing their predicted and actual proteasome-inhibitory activities.

MATERIALS AND METHODS

Materials

Highly purified tea polyphenols (−)-EGCG (>95%), (−)-GCG (>98%), (−)-ECG (>98%) and (−)-CG (>98%) were purchased from Sigma (St. Louis, MO). (+)-EGCG, benzyl-protected-(+)-EGCG, (+)-GCG, (−)-EGCG-amide, and (+)-EGCG-amide were prepared by enantioselective synthesis (see below). Purified 20S eukaryotic proteasome from rabbit was purchased from Boston Biochem (Cambridge, MA). Purified 20S prokaryotic proteasome (*Methanosarcina thermophile*, recombinant, *E. coli*) was purchased from Calbiochem (La Jolla, CA). Fluorogenic peptide substrates Suc-Leu-Leu-Val-Tyr-AMC (for the proteasomal chymotrypsin-like activity) was obtained from Calbiochem (La Jolla, CA).

Enantioselective Synthesis of GTPs

Synthesis of (+)-EGCG, benzyl-protected-(+)-EGCG, and (+)-GCG were as described previously.[29] The chemical synthesis of (−)-EGCG-amide and (+)-EGCG-amide starting from trans-5,7-bis-benzyloxy-2-[3,4,5-tris (benzyloxy)-phenyl] chroman-3-ol[29,30] will be published elsewhere separately.

Inhibition of Purified 20S Proteasome Activity by Natural or Synthetic GTPs

The chymotrypsin-like activity of purified 20S proteasome was measured as previously described.[28] Briefly, purified prokaryotic (0.5 μg) or eukaryotic (0.02 μg) 20S proteasome was incubated with 20 μM fluorogenic peptide substrate, Suc-Leu-Leu-Val-Tyr-AMC for 30 min at 37°C in 100 μL of assay buffer (50 mM Tris-HCl, pH 7.5), with or without a natural or synthetic tea polyphenol. After incubation, production of hydrolyzed 7-amido-4-methyl-coumarin (AMC) groups was measured by using a multiwell plate VersaFluor™ Fluorometer with an excitation filter of 380 nm and an emission filter of 460 nm (Bio-Rad).

Assays for Irreversible Inhibition

To measure the effect of dialysis on (−)-EGCG-mediated proteasome inhibition, 20S prokaryotic proteasome (2 μg) was incubated with 10 μM (−)-EGCG or the control solvent (H_2O) in 50 mM Tris-HCl, pH 7.5 for 1 h. This was then incubated at 4°C either without or with dialysis overnight using a 10,000 MWCO Pierce Slide-A-Lyzer Dialysis Cassette (Rockford, IL) in a rotating bath

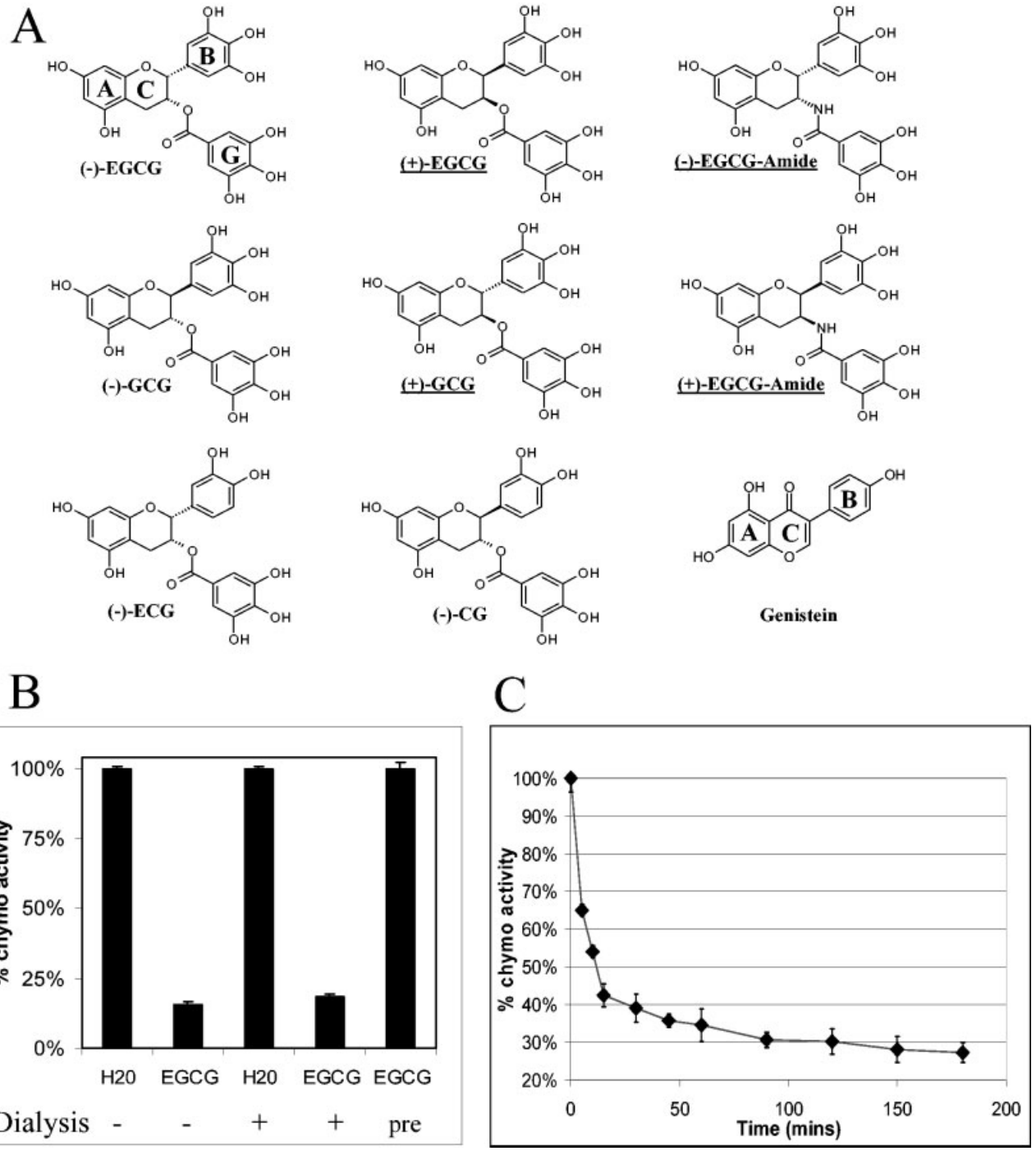

Fig. 1. Structures of GTPs and irreversible inhibition of 20S proteasome activity by (−)-EGCG. **A:** Structures of the natural and synthetic GTPs. The names of the synthetic GTPs are underlined to distinguish them from the natural compounds. The ring nomenclature was defined as A, C, B, or G (for gallate) rings[41] and used throughout the text. **B:** Dialysis does not affect (−)-EGCG-mediated proteasome inhibition. The purified 20S prokaryotic proteasome (2 μg) was incubated overnight at 4°C in the presence or absence of 10 μM (−)-EGCG, with or without dialysis. Percentage of chymotrypsin (chymo) activity was then determined. The prokaryotic proteasome was used because it showed more stable kinetics after overnight dialysis, although similar result could be obtained with eukaryotic proteasome (data not shown). **C:** Kinetics of (−)-EGCG-mediated proteasome inhibition. (−)-EGCG at 1 μM was incubated with eukaryotic 20S proteasome (0.02 μg) and suc-LLVY-AMC (20 μM) for the indicated times, followed by measurement of the chymotrypsin activity. Values are means from four independent experiments, and error bars represent standard deviations.

of 50 mM Tris-HCl, pH 7.5. The proteasomal chymotrypsin-like activity was then assayed as previously described.[28] As a control, an EGCG solution (without purified 20S proteasome) was dialyzed overnight, followed by measurement of the effects on inhibition of the proteasome activity.

TABLE I. Relative Cluster Rank and Docked Free Energies of Selected Docking Modes

Compound	Number of AutoDock clusters[a]	Cluster rank[b] of selected docked structure[c]	Docked free energy range of docked structures[d]	Docked free energy of selected docked structure[d]
(+)-EGCG	8 (10)	1	−10.82 to −8.75	−10.82
(−)-EGCG	4 (5)	2	−10.62 to −9.83	−10.52
(+)-GCG	3 (5)	3	−12.39 to −10.33	−10.33
(−)-ECG	15 (30)	2	−10.81 to −8.34	−10.56
(−)-EGCG-A	23 (30)	8	−11.38 to −8.23	−9.63
(+)-EGCG-A	5 (5)	4	−11.70 to −9.28	−9.52
(−)-CG	19 (30)	7	−10.46 to −7.93	−9.30
(−)-GCG	22 (30)	13	−10.27 to −7.24	−9.10
genistein	12 (100)	4	−5.40 to −4.23	−5.15

[a]Number of GA runs are shown in parentheses
[b]The cluster rank is the absolute ranking as determined by the docked free energy defined by AutoDock.
[c]The criteria used for selection were as follows: (1) distance between the ester carbonyl carbon of the compound and hydroxyl oxygen of Thr1 and 2) the A–C ring system located in the S1 pocket.
[d]kcal/mol.

Molecular Modeling and Docking Studies

The crystal structure of the eukaryotic yeast 20S proteasome was obtained from the Protein Database[31] (Ref. number 1JD2) and used for all the docking studies presented here. The yeast 20S proteasome is structurally very similar to the mammalian 20S proteasome, and the chymotrypsin active site between the two species is highly conserved.[2,4] The AutoDock 3.0 suite of programs, which was used for the docking calculations, uses an automated docking approach that allows ligand flexibility as described to a full extent elsewhere.[32] AutoDock has been compared with various docking programs in several studies and has been found to be able to locate docking modes that are consistent with X-ray crystal structures.[33,34] Default parameters (including a distance-dependent dielectric "constant") were used as described in the AutoDock manual except for those changes mentioned below. The dockings were run on an i386 architecture computer running Redhat Linux 6.0. The crystal structure of the 20S proteasome and the ligands were prepared for docking by following the default protocols except where noted. The energy-scoring grid was prepared as a $20 \times 20 \times 20$ Å box centered around the β5-catalytic N-terminal threonine, and the ligand was limited to this search space during docking. Atomic solvation parameters were assigned to the proteasome using default parameters. The default parameters for the Lamarckian genetic algorithm[32] were used as the search protocol except for the maximum number of energy evaluations, which were changed to 5 million (the population size was retained at 50). AutoDock relies on an empirical scoring function, which provides approximate binding free energies. AutoDock reports a docked energy that we have referred to in this article as a "docked free energy" because it includes a solvation free energy term. The docked energy also includes the ligand internal energy or the intramolecular interaction energy of the ligand. AutoDock also reports a binding free energy that excludes the ligand internal energy but includes a torsional free energy term for the ligand based on the number of rotatable bonds.

In the present study, we chose to use the docked free energies because the number of rotatable bonds in our inhibitors is relatively constant and because we believed that the internal energy of the ligand should not be neglected for our compounds. Its neglect is tantamount to assuming that the intramolecular interaction energy of the ligand is the same in the complex as in solution. It is worth noting that the docked free energies (or binding free energies) that one obtains may vary, depending on the precise force field parameters in use (e.g., charges, electrostatic treatment, etc.). For the GA algorithm, the default parameters were kept for mutation, crossover, and elitism. The pseudo-Solis and Wets local search method was included by using default parameters as well. Docking modes were selected on the basis of two criteria: their proximity to the N-terminal threonine and placement of the A-C ring system of the molecule within the S1 hydrophobic pocket. Of the orientations/conformations that fit these two criteria, the docked structure of lowest docked free energy was chosen. Each molecule was docked with up to 30 genetic algorithm runs of 5 million energy evaluations for each run. AutoDock reports the best docking solution (lowest docked free energy) for each GA run and also performs a cluster analysis in which the total number of clusters and the rank of each docking mode (cluster rank) is reported. So, for a 30 GA run, for example, there would be up to 30 total docking modes from which we then selected the lowest energy-docking mode that met the two criteria. In Table I, we indicate the number of clusters for each compound docked, the cluster rank of the docking mode selected, the range of docked free energies, and the docked free energy of the docking mode selected. It should be noted that for most of the GTPs docked, only docking modes from a single cluster met both of the two preset criteria, and the docking mode with the lowest docked free energy was selected from this cluster. The output from AutoDock and all modeling studies as well as images were rendered with PyMOL.[35] PyMOL was used to calculate the distances of hydrogen bonds as measured between the hydrogen and its assumed binding partner.

Determination of Nucleophilic Susceptibility

The electron density surface colored by nucleophilic susceptibility was created by performing Extended Hückel molecular orbital calculations with use of CaChe Worksystem version 3.2 (Oxford Molecular Ltd., now Accelrys), as described previously.[28] A colored "bull's-eye" with a white center denotes atoms that are highly susceptible to nucleophilic attack.

RESULTS AND DISCUSSION

(−)-EGCG Irreversibly Inhibits the Chymotrypsin-Like Activity of Purified 20S Proteasome

To investigate the nature of (−)-EGCG-mediated proteasome inhibition,[28] we performed a dialysis experiment. A purified prokaryotic 20S proteasome (*Methanosarcina thermophile*, recombinant *E. coli*) was preincubated for 1 h at 37° C with either 10 μM (−)-EGCG or its control solvent (H_2O), followed by overnight coincubation at 4°C with or without dialysis. Figure 1(B) shows that in the absence of dialysis, (−)-EGCG was able to inhibit the chymotrypsin-like activity of the prokaryotic 20S proteasome by 85%. More importantly, overnight dialysis of the EGCG-proteasome mixture did not change the outcome: (−)-EGCG still caused 81% inhibition of the proteasomal chymotrypsin-like activity. As a control, when an aliquot of (−)-EGCG was first dialyzed overnight and then added to the purified 20S proteasome, no inhibition was observed [Fig. 1(B), EGCG pre]. This result shows that (−)-EGCG is either an irreversible or a tight-binding inhibitor of the chymotrypsin-like activity of the proteasome.

We also performed a kinetics experiment. (−)-EGCG at 1 μM potently inhibited the chymotrypsin-like activity of a purified eukaryotic (rabbit) 20S proteasome in a time-dependent manner: 35% at 5 min, 62% at 30 min, and 70–80% after 1–3 h [Fig. 1(C)], which is characteristic for a mechanism-based inhibitor.[36] This result further supports the argument that the mode of (−)-EGCG action is irreversible inhibition.

Previously, we hypothesized that (−)-EGCG's susceptibility to a nucleophilic attack would be essential for inhibiting the proteasome.[28] This hypothesis was further supported by our HPLC results that showed that the proteasome could attack and degrade (−)-EGCG.[28] Kinetic analysis[37] and X-ray diffraction[2] studies using the specific proteasome inhibitor lactacystin have shown that the ester bond of this inhibitor covalently modifies the N-terminal threonine of the β5-subunit, which is critical for proteasome inhibition.[4] Because (−)-EGCG contains an ester bond[28] [Fig. 1(A)] and inhibits the proteasome irreversibly in a time-dependent manner [Fig. 1(B) and (C)], it is probable that a lactacystin-like reaction occurs with (−)-EGCG.

Automated Docking of (−)-EGCG to the β5-Subunit of 20S Proteasome

To build a model for how (−)-EGCG binds to the proteasome, which will allow for nucleophilic attack, we performed automated docking studies. Knowledge of the enzyme kinetics discussed above can help direct docking solutions that would allow covalent modification and inhibition of the proteasome. Before acylation of Thr 1's hydroxyl by (−)-EGCG can occur, (−)-EGCG must bind to the β5-active site in a conformation that would allow a reaction to occur between the two atoms involved. Therefore, binding of (−)-EGCG in an appropriate orientation and conformation is necessary[38] for ester bond scission because the presence of an ester bond alone is insufficient to inhibit the proteasome. This finding is shown by benzyl protected-EGCG, which has an ester-bond, but cannot inhibit the proteasome.[29] In addition, several small molecular weight molecules that contain ester bonds, including methyl acetate, benzyl hydroxybenzoate, and methyl gallate, cannot inhibit the proteasome (unpublished observations).

Therefore, docking modes were chosen on the basis of the following two predefined criteria. First, the distance between the carbonyl carbon of (−)-EGCG and the hydroxyl oxygen of Thr 1 must be between 3 and 4 Å.[39] Second, the A-C ring system must be located within the S1 pocket (for details, see Materials and Methods). On the basis of these two criteria, the lowest docked free energy (negative ΔG) was chosen for such a bound conformation.[40] After docking (−)-EGCG to the β5-chymotrypsin active site using five separate genetic algorithm runs, the ester bond of (−)-EGCG in one of the two lowest docked free energy structures could be easily found oriented directly over the Thr 1 side-chain and the ester bond-carbon was located 3.18 Å away from the hydroxyl of Thr 1 [Figs. 2(A) and (B)]. Such an orientation/conformation of the inhibitor is well suited for nucleophilic attack and is structurally achievable, which satisfies the first predefined criterion. In addition, the fairly hydrophobic A-C rings of (−)-EGCG [see Fig. 1(A)] were oriented in the S1 pocket of the β5-subunit, the B ring projected up into solvent, bridging the two walls of the binding cleft, and the gallate (G) group sat above Ser 131 [Figs. 2(A) and 3(A)]. (−)-EGCG filled most of the binding cleft, which was seen by drawing a water-accessible mesh surface around (−)-EGCG when docked into the binding site as depicted by a ribbon structure of the β5-subunit [Figs. 2(B) and (C)]. The occupancy of the S1 pocket satisfied the second criterion, and the docking mode chosen possessed a docked free energy of −10.52 kcal/mol with a range of docked free

Fig. 2. Docking solution of (−)-EGCG. (−)-EGCG was docked to the chymotrypsin active site (β5) of the yeast 20S proteasome allowing ligand flexibility (see Materials and Methods for details). This docking mode was chosen on the basis of the two criteria set in Results and Discussion. **A:** A stick figure of (−)-EGCG with a transparent surface is used to show the proximity between (−)-EGCG and the N-terminal Threonine (Thr 1, represented by a space-filling model). The dotted yellow line represents a distance of 3.18 Å from the hydroxyl of Thr 1 to the carbonyl carbon of (−)-EGCG. **B:** Another view is given of this interaction with a mesh surface drawn around (−)-EGCG and the Thr 1 represented in sticks. Red is used for oxygen, blue for nitrogen, gray for carbon, and white for hydrogen. **C:** An overview of (−)-EGCG's binding mode to the β5-subunit is also shown. (−)-EGCG is represented by stick model with a mesh surface, bound to the β5-binding cleft (ribbon representation). **D:** Noncovalent interaction between the β5-subunit and (−)-EGCG. The S1 hydrophobic pocket is layered with a transparent surface, and residues that interact hydrophobically are given along with distances from the residue to the A-C rings in (−)-EGCG.

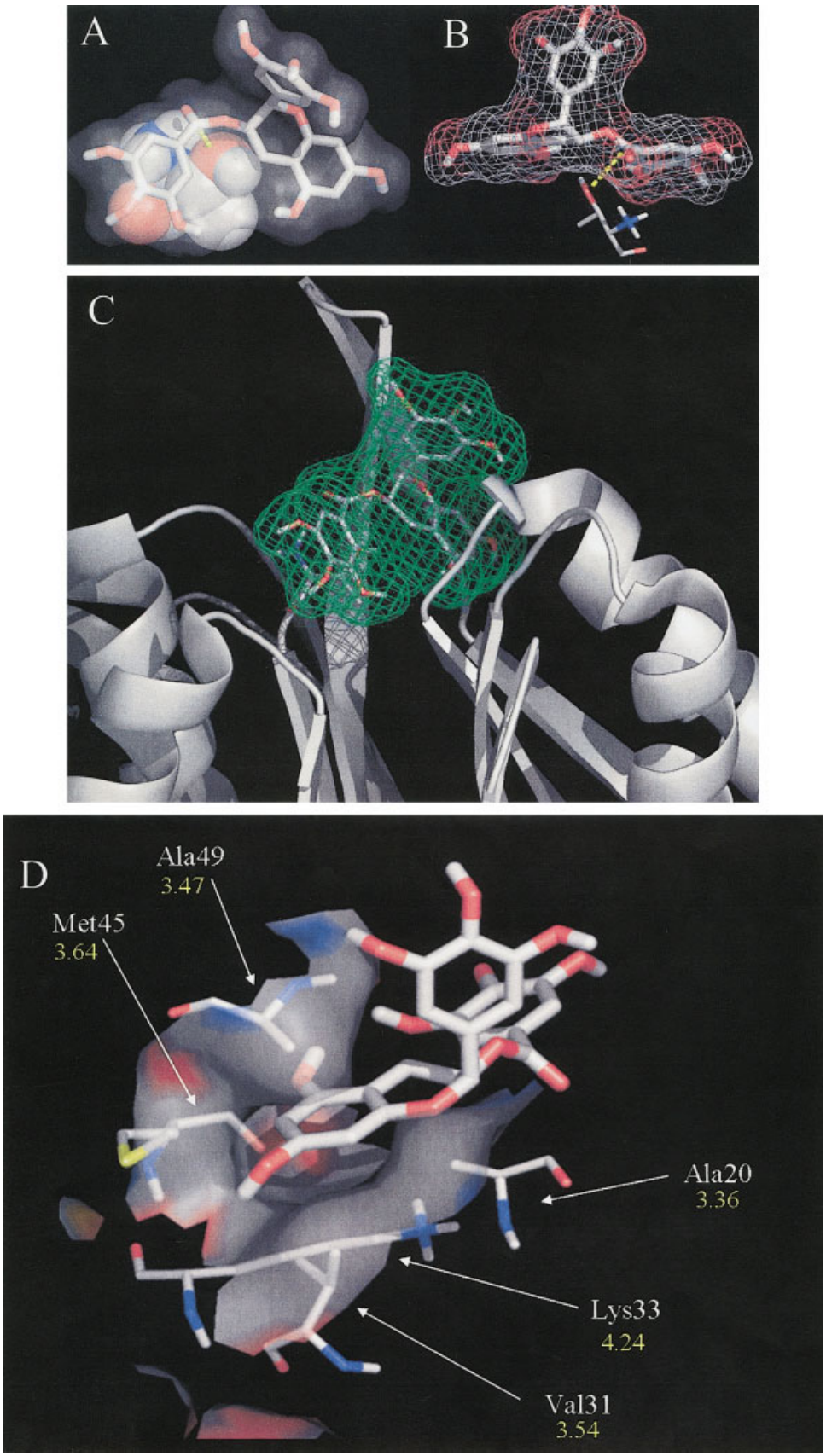

Figure 2.

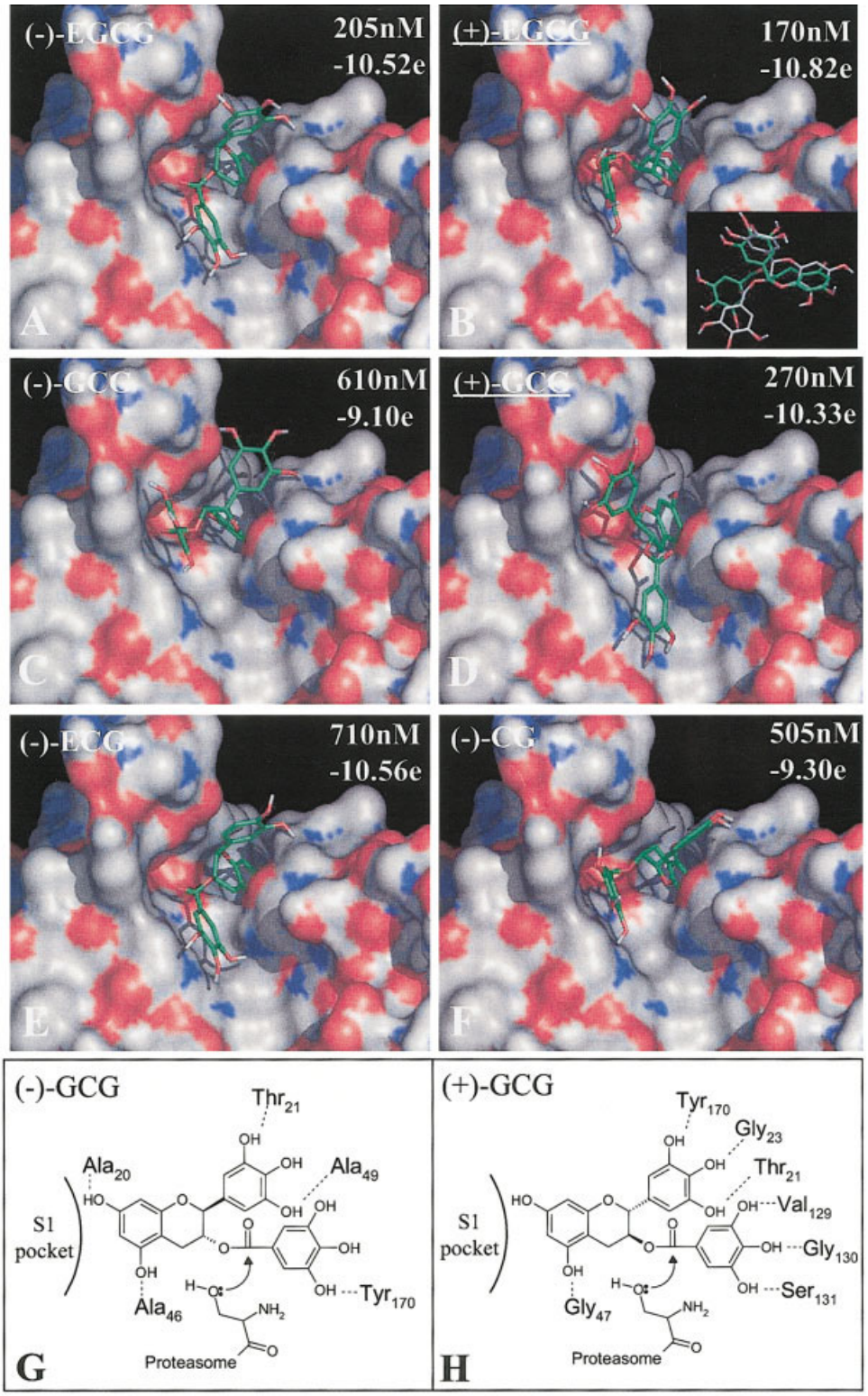

Fig. 3. Binding modes of EGCG analogs. Each EGCG analog is represented by stick structure (see also Fig. 2 for description) with their names in top left corner (underlined names are synthetic analogs). The IC_{50} values (in nM) to the chymotrypsin-like activity of purified rabbit 20S proteasome are listed in the top right corner, along with the docked free energy value (e = kcal/mol, used to score each docking mode) calculated from the final docked conformations of each respective analog. Similar results for IC_{50} values were obtained in six or more independent experiments. For (+)-EGCG inset (**B**), an overlap of (−)-EGCG and (+)-EGCG (green) binding modes is shown. The β5-subunit is represented with a water accessible surface and colored by atom type (O-red, N-blue, C-gray, and H-gray). A two-dimensional scheme for (−)-GCG and (+)-GCG is given (**G,H**). The dotted lines represent potential hydrogen bond formations and the S1 pocket designation represents hydrophobic interactions (G, H).

energies between −9.83 and −10.62 kcal/mol (see Table I). Moreover, the second lowest docked free energy structure met all the criteria described above. This resultant model supports the hypothesis that (−)-EGCG first binds to the β5-active site and then is attacked by the N-terminal threonine, rendering the proteasome inactive by acylation.

To look further into the favorable binding mode of (−)-EGCG to the proteasomal chymotrypsin active site, we analyzed hydrogen-bond (H-bond) formation. There are eight polar hydrogens and one carbonyl-oxygen on (−)-EGCG that are available for H-bonding [see Fig. 1(A)]. It appears that all but two of these sites are capable of actively participating in H-bonding (docked structure not shown). It should be noted that we used a relatively loose criterion to establish the presence of a hydrogen bond. Consistent with this prediction, the fully benzyl protected-EGCG without free OH groups, which should not form H-bonds, fails to inhibit the proteasome[29] and could not be found docked in an orientation/conformation that met criteria 1 and 2 (docked structure not shown).

We then analyzed the hydrophobic interactions between (−)-EGCG and the β5-subunit. The chymotrypsin-like activity of the proteasome cleaves peptides after hydrophobic residues, such as the Tyr in the model fluorogenic substrate Suc-Leu-Leu-Val-Tyr-AMC. This Tyr would bind to the S1 hydrophobic pocket of the β5-subunit to allow for specific chymotrypsin-like cleavage of the AMC group. It seems that the A ring of (−)-EGCG mimics the Tyr residue of the proteasome peptide substrate: the hydrophobic portion of this aromatic ring is oriented in the middle of the S1 pocket between the side-chains of Ala 49, Ala 20, and Lys 33 [with distances of 3.47, 3.36, and 4.24 Å, respectively; Fig. 2(D)]. This conformation would allow the hydrophilic hydroxyls of the A ring to project out of the two sides of the S1 hydrophobic pocket and participate in H-bonding. In addition, the sidewalls of the S1 pocket that interact with (−)-EGCG are created by Met 45 and Val 31 [3.64 and 3.54 Å; Fig. 2(D)]. Each of these hydrophobic or partially hydrophobic residues are <4.5 Å from (−)-EGCG [see Fig 2(D)], suggesting that entropically driven hydrophobic interactions might indeed occur between the (−)-EGCG A-C rings and the S1 pocket. Therefore, inhibition kinetics, along with docking studies of (−)-EGCG bound to the proteasome β5-subunit, suggests a mechanistic model for how (−)-EGCG inhibits the proteasomal chymotrypsin-like activity.

Docking of Other Natural and Synthetic EGCG Analogs

We next investigated whether this established model of (−)-EGCG inhibition could also be used to interpret the proteasome-inhibitory properties of other EGCG analogs. Three natural, (−)-GCG, (−)-ECG, and (−)-CG, and two synthetic, (+)-EGCG and (+)-GCG, polyphenols were chosen, all of which contain an ester bond [Fig. 1(A)]. We found that, similar to (−)-EGCG, all of these five polyphenols potently inhibited the chymotrypsin-like activity of the rabbit 20S proteasome, with IC_{50} values similar to those obtained by using prokaryotic 20S proteasome (Table II and Fig. 3 vs Refs. 28 and 29).

TABLE II. Predicted Versus Observed Docked Free Energies

Compound	Predicted ΔG° (kcal/mol)	IC_{50}	$-RT \ln(1/IC_{50})$[a]
(+)-EGCG	−10.82	170 nM	−9.60
(−)-EGCG	−10.52	205 nM	−9.49
(+)-GCG	−10.33	270 nM	−9.32
(−)-ECG	−10.56	710 nM	−8.72
(−)-EGCG-A	−9.63	320 nM	−9.21
(+)-EGCG-A	−9.52	405 nM	−9.07
(−)-CG	−9.30	505 nM	−8.93
(−)-GCG	−9.10	610 nM	−8.81
genistein	−5.15	26 μM	−6.50

[a]Note that IC_{50} is proportional to K_i. Because K_i is the equilibrium constant for the dissociation of the enzyme-inhibitor complex, and the free energy (ΔG°) is related to the equilibrium constant for the association of enzyme with inhibitor, ΔG° is proportional to $-RT \ln(1/IC_{50})$, which is identical to $+RT \ln(IC_{50})$.

We then docked each of these five polyphenols to the 20S proteasome β5-subunit by using (−)-EGCG as a comparison (Fig. 3). For each compound (plus the two amide analogs, see below and Fig. 4), a single docking mode with the lowest docked free energy was selected after applying the two preset criteria (Table I). For each of these compounds, it was possible to locate a viable docking mode (based on the two criteria previously described) with as few as five GA runs. In many instances, the selected docking mode was a member of a cluster of high rank (i.e., possessed a docked free energy that was low relative to the global minimum docked free energy structure).

In our docking studies, (+)-EGCG was found to be slightly more potent than (−)-EGCG with regard to purified 20S proteasome [IC_{50} 170 nM vs 205 nM; Figs. 3(A) and (B)]. (+)-EGCG was oriented in the proteasome β5-subunit with a seemingly similar mode compared to (−)-EGCG, with the A-C rings in the S1 pocket and the B ring in solvent, bridging the binding cleft [Fig. 3(B) vs (A)]. The ester bond-carbon (and gallate group) was shifted only 0.38 Å away from Thr 1 but still resided over Thr 1 in a suitable position for a nucleophilic attack [see Fig. 3(B), inset, for overlap of (+)-EGCG and (−)-EGCG]. The shift of this gallate group placed the carbonyl oxygen into the binding cavity created by Arg 19 and Thr 21, allowing for an increased van der Waals interaction and a slightly more favorable docked free energy [−10.82 kcal/mol vs −10.52 kcal/mol; Figs. 3(A) and (B)], explaining the increased activity of this compound. A closer inspection revealed that (+)-EGCG had to flip >180° (in relation to the plane of the A-C rings) to attain a similar orientation/conformation. It is known that (−)-EGCG and (+)-EGCG have (*2R, 3R*) and (*2S, 3S*) stereochemistry, respectively [Fig. 1(A)]. This finding suggests that if the B ring and the gallate group of (+)-EGCG were to bind in the same position in three-dimensional space as (−)-EGCG, the A-C rings of (+)-EGCG would then have to rotate 180° to compensate [see inset, Fig. 3(B)]. The model suggests that proteasome does

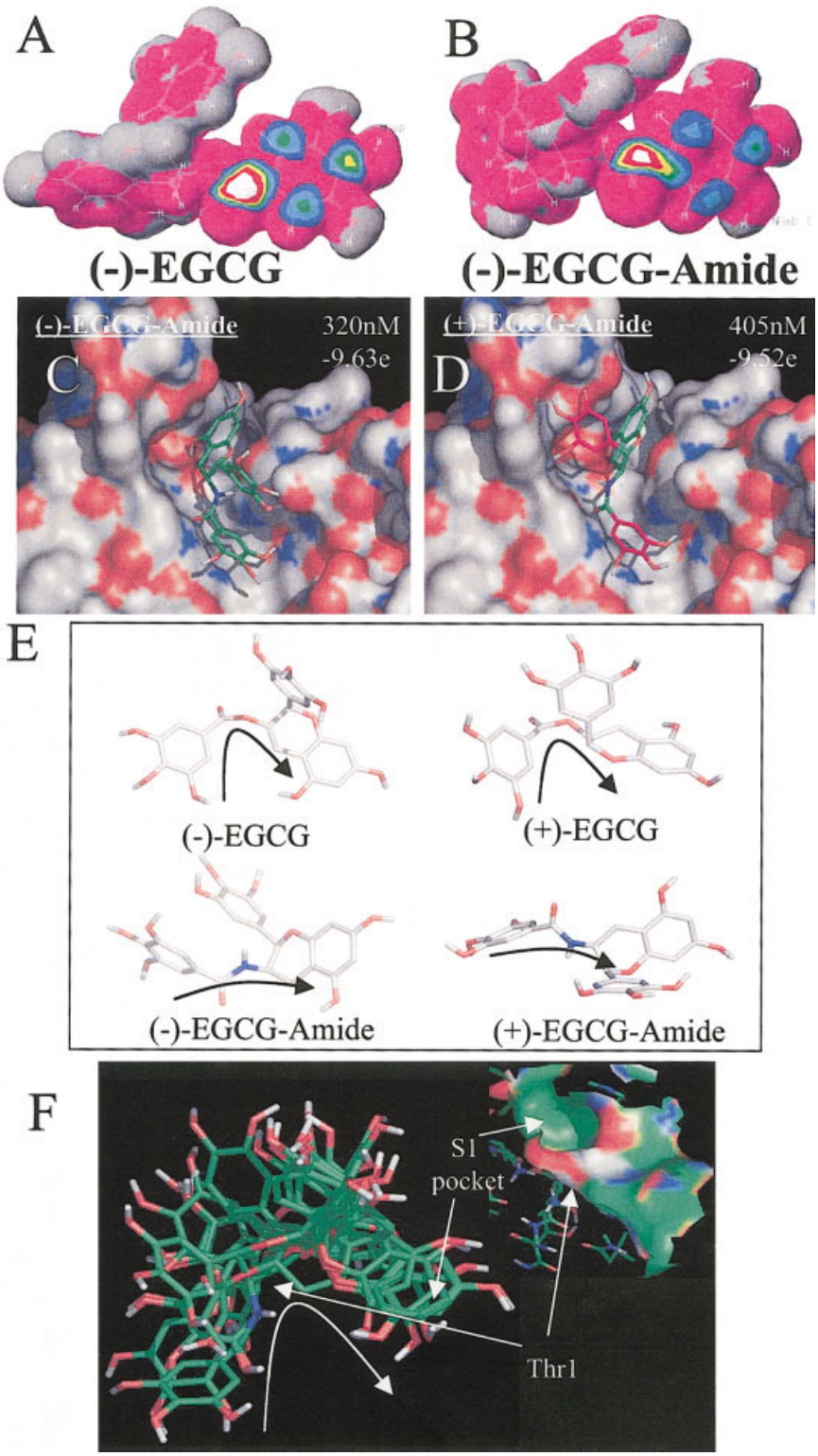

Figure 4. (Continued on next page.)

not exhibit significant enantioselectivity for EGCG[29] (Fig. 3) due to the partial symmetry of the A-C rings.

(−)-GCG is a non-"*epi*" compound that has *trans* stereochemistry about the C ring, unlike (−)-EGCG which has *cis* stereochemistry [Fig. 1(A)]. The IC_{50} value of (−)-GCG indicates that it is nearly 3 times less potent than (−)-EGCG (610 nM vs 205 nM; Figs. 3(A) and (C), suggesting that the *trans* stereochemistry may not be as beneficial for

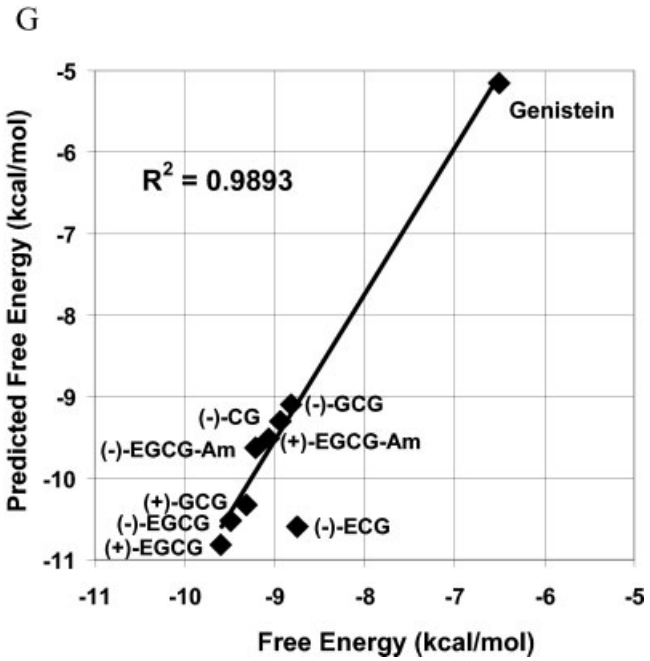

Fig. 4. (Continued) Decreased nucleophilic susceptibility and ester bond flexibility in EGCG amides are associated with decreased proteasome-inhibitory activity. **A,B:** The nucleophilic susceptibility of (−)-EGCG and (−)-EGCG amides. Molecular orbital energy analysis is shown by drawing an electron density isosurface and coloring by nucleophilic susceptibly.[28] The white center signifies the highest area of susceptibility. **C,D:** Binding modes of (−)-EGCG-amide and (+)-EGCG-amide. Also see Figure 3. **E:** The bound conformation of EGCG and their amides are given along with arrows to trace the saddle conformation formed with the ester bonds in (−)- and (+)-EGCG and the linear amide bonds in (−)- and (+)-EGCG-amide compounds. **F:** An overlap of all the eight bound ligands (Figs. 3 and 4) are given along with a view of the bottom of the saddle-shaped binding pocket (occluding residues have been removed) with surface colored by atom type. The S1 pocket and Thr 1 are designated. **G:** The calculated docked free energy predicts the actual proteasome-inhibitory activity. A plot of predicted docked free energy (in kcal/mol) against the actual proteasome-inhibitory activity (converted from IC_{50} values to kcal/mol; see below). A regression analysis R^2 value for a best-fit line was 0.9893 [without (−)-ECG; see text]. IC_{50} values of each compound were used in the formula, -RT[ln(1/IC50)]. Here the value used for R (gas constant) was 0.0019872 kcal/K*mol and T was 310 K (the temperature of the experiment was 37°C). These values were then plotted against the ΔG values computed by AutoDock in the docking process. Also see Table II.

binding to the proteasome's active site. In agreement with the experimental IC_{50} values, the calculated docked free energy of (−)-GCG was −9.10 kcal/mol [Fig. 3(C)] compared with −10.52 kcal/mol for (−)-EGCG [Fig. 3(A)]. For clarity, a two-dimensional scheme of the binding mode for (−)-GCG is also represented [Fig. 3(G)].

The synthetic (+)-GCG was more potent than the natural (−)-GCG [270 nM vs 610 nM; Figs. 3(C) and (D)]. Consistent with their IC_{50} values, a lower docked free energy is obtained for the binding of (+)-GCG to β5-subunit compared to (−)-GCG (−10.33 kcal/mol vs −9.10 kcal/mol; Figs. 3(C) and (D). (+)-GCG binds in a slightly different conformation compared with the rest of the other compounds [Fig. 3(H)]. The unique (+)-*trans* stereochemistry of (+)-GCG allows for its B ring to potentially form three H-bonds instead of two as with (−)-EGCG. It also hydrophobically interacts with Tyr 170 [see Fig. 3(H)], which has stronger affinity than the binding cleft bridging conformation. The gallate group of (+)-GCG also extends farther out of the pocket and is available to form three potential H-bonds [Figs. 3(D) and (H), instead of the two potential H-bonds as with (−)-EGCG. However, although this conformation may increase binding affinities at the B ring and gallate moieties, the A-C rings are pulled slightly out of the S1 pocket, reducing the total number of potential interactions that could take place. As a net result, a slight overall increase in docked free energy and a slight reduction in in vitro proteasome-inhibitory activity occurs, compared to (−)-EGCG [Fig. 3(D) vs (A)].

The natural GTP (−)-ECG lacks one hydroxyl group on its B ring [Fig. 1(A)], which significantly reduces its solubility in water and also decreases its potency against 20S proteasome by more than threefold, compared to (−)-EGCG [710 nM vs 205 nM; Figs. 3(A) and (E)]. (−)-ECG is also found to bind the β5-binding cleft with almost exactly the same binding mode as (−)-EGCG [Fig. 3(E) vs (A)]. However, this did not increase the calculated docked free energy (−10.56 vs −10.52 kcal/mol). Because the B ring is protruding into solvent and, as mentioned previously, the loss of this hydroxyl significantly decreases the solubility of (−)-ECG, binding of this GTP to the proteasome might be affected in a manner that is not well accounted for by the solvation model used in the docking algorithms.

The natural GTP (−)-CG is another non-*epi* compound with a *trans* stereochemistry [Fig. 1(A)] and is less potent than (−)-EGCG [Fig. 3(F) vs (A)]. Consistent with this finding, a significantly increased ligand internal energy [+0.42 kcal/mol for (−)-CG vs ≤0.38 kcal/mol for (−)-EGCG] is calculated for binding of (−)-CG to the proteasome's active site, thereby giving a net increase in docked free energy [−9.30 kcal/mol vs −10.52 kcal/mol; and see the discussion about (−)-GCG].

To test whether the developed computational model can be applied to a range of compounds with different chemical structures, we selected genistein, the predominant isoflavone found in soy products. Like (−)-EGCG, genistein also consists of a ring system similar to the A, C, and B rings of the GTPs [see Fig. 1(A), suggesting that genistein might be a proteasome inhibitor. But different from (−)-EGCG, genistein lacks the gallate group [see Fig. 1(A)], which suggests that genistein would be less potent than (−)-EGCG. To test this hypothesis, we first docked genistein to yeast 20S proteasome. We found that in 60 of 100 runs with 5 million energy evaluations, genistein docks primarily in the S1 pocket of the active site of the proteasome β5-subunit (Table I). The B ring hydroxyl group of genistein lies in close proximity to Thr 1, and up to four potential hydrogen bonds could be formed within the complex of genistein and the proteasomal β5-subunit (docking modes not shown). However, the docked free energy of genistein to β5-subunit was found to be −5.15 kcal/mol (Table I), much higher than that of (−)-EGCG [−10.52 kcal/mol; Fig. 3(A)]. Consistent with its higher docked free energy, genistein weakly inhibits the chymotrypsin-like activity of purified 20S proteasome with an IC_{50} value of 26 μM [also

see Table II and Fig. 4(G)], in contrast to an IC_{50} of 205 nM for (−)-EGCG [Fig. 3(A)]. These data further support the conclusion that our established computational model could satisfactorily describe the EGCG-β5-interaction that is responsible for its proteasome-inhibitory activity.

Rational Design, Synthesis, and Validation of EGCG-Amides as Proteasome Inhibitors

To further test the model of proteasome inhibition by EGCG analogs, we decided to rationally design related compounds and examine whether they possess the expected properties as predicted by the in silico docking studies. We hypothesized that an EGCG analog with altered nucleophilic susceptibility to the ester bond-carbon would have altered proteasome-inhibitory potency. For example, replacement of the ester bond-oxygen of EGCG with nitrogen (EGCG-amide) would render the carbonyl functional group less susceptible to a nucleophilic attack due to the presence of the amide nitrogen. Indeed, as expected, molecular orbital calculations confirmed that the ester bond-carbon of (−)-EGCG produced an arbitrary value of 0.69 for nucleophilic susceptibility, whereas the same carbon in (−)-EGCG-amide had a value of 0.55 [Figs. 4(A) and (B)].[28]

To determine whether the reduction in nucleophilic susceptibility would result in a decreased potency to inhibit the proteasome activity, we synthesized (−)-EGCG-amide and (+)-EGCG-amide [Fig. 1(A)]. The IC_{50} values against 20S eukaryotic proteasome were determined to be 320 and 405 nM for both (−)-EGCG-amide and (+)-EGCG-amide, respectively [Figs. 4(C) and (D)]. Compared to (−)- and (+)-EGCG, both amide compounds have decreased proteasome-inhibitory potencies, respectively [Figs. 4(C) and (D) vs Figs. 3(A) and (B)], although their stereochemical structures were not changed [Fig. 1(A)]. This finding suggests that reduction in nucleophilic susceptibility is indeed associated with decreased potency to inhibit 20S proteasome activity, as predicted by the model.

It is of interest that the molecular modeling studies with the amide compounds brought another property of (−)-EGCG inhibition to light. When (−)-EGCG binds the proteasome, a saddle shape is formed between the A-C rings extending past the ester bond and back down to the gallate moiety [Fig. 4(E)]. The more flexible nature of the ester bond allows this conformation to occur so that (−)-EGCG might fit the saddle shape formed by the bottom of the binding pocket [Fig. 4(F), top/right). In fact, when the docked conformations of all the EGCG analogs are overlapped into one image, this saddle shape can be easily observed [Fig. 4(F)]. It can be assumed that this saddle-shaped conformation of EGCG would also place additional strain on the scissile bond, further lowering the activation energy for nucleophilic attack. However, introduction of a nitrogen atom into EGCG, as in EGCG-amide, reduces bond flexibility. It is well known that such an amide bond (or peptide bond) is less flexible than the ester bond and prefers the trans conformation. Therefore, because of the decreased flexibility of the amide bond, the amide polyphenols cannot adopt a saddle-shaped conformation that is energetically favorable for binding. This causes a straightening out of the arch conformation [Fig. 4(E)], which does not allow the A-C rings to bind as deeply in the S1 pocket as (−)-EGCG, thus pulling the compound farther out of the binding cleft. This consequently raises the docked free energy of both (−)-EGCG-amide and (+)-EGCG-amide [−9.63 and −9.52 kcal/mol, respectively; Figs. 4(C) and (D)]. This binding mode with increased docked free energy agrees with the increase in the IC_{50} values of both amide compounds (Fig. 4) and may (along with their reduced nucleophilic susceptibility) explain their decreased potency relative to the corresponding esters. Consistent with the prediction that EGCG-amides are also irreversible or tight-binding proteasome inhibitors, we found that the amide analogs were able to accumulate levels of the proteasome target protein p27 in breast cancer MCF-7 cells, with potency comparable to that of (−)-EGCG (unpublished data).

Finally, to compare the selected binding modes to the actual proteasome-inhibitory activities of each of the eight EGCG analogs and genistein, we plotted the predicted activity (docked-free energy) against the actual inhibitory activity (IC_{50} values; converted to kcal/mol) [Table II and Fig. 4(G)]. A decrease in the docking free energy for eight of the nine compounds was correlated with an increase in the actual activity of each of these compounds. Only one compound, (−)-ECG, did not fit the linear relationship between the predicted and actual activity [Fig. 4(G)]. This significant loss in actual activity of (−)-ECG, which is not in congruence with the calculated docked free energy, may be due to the orientation and solvation issues mentioned previously. A regression analysis R^2 value of 0.9893 was determined for a best-fit line, not including the values generated for (−)-ECG. These data support our model of proteasome inhibition by EGCG analogs.

CONCLUSION

There are two aspects of proteasome inhibition by (−)-EGCG. First, it was shown that (−)-EGCG irreversibly inhibits the chymotrypsin-like activity of the proteasome in a time-dependent manner (Figs. 1(B) and (C)], so it is plausible that a nucleophilic attack of the ester bond-carbon of (−)-EGCG occurs. Second, for the above event to occur, (−)-EGCG must bind to the active site in such a mode that allows for attack of the carbonyl carbon of (−)-EGCG to take place [Fig. 2(A)]. Our established model suggests that any analogs of (−)-EGCG that bind (with reasonable affinity) to the active site in an orientation/conformation more conducive to nucleophilic attack should produce a higher rate of attack and thus greater inhibition. In contrast, those analogs that bind to the active site in an orientation/conformation less favorable for nucleophilic attack should produce a lower rate of attack and thus less inhibition. Of course, it is possible that one could have a molecule that binds tightly to the enzyme but is not in an orientation/conformation favorable for nucleophilic attack. This molecule may very well inhibit the enzyme, but not irreversibly through acylation.

(−)-EGCG can bind the proteasome's chymotrypsin active site in an orientation and conformation that is well suited for nucleophilic attack as described by the following model. First, favorable hydrophobic surface interactions exist (tyrosine-like mimic in S1 pocket) [Fig. 2(D)]. Second, there is a large potential van der Walls contact surface area [Fig. 2(C)]. Third, the calculated docked free energy values are favorable for binding of (−)-EGCG to the proteasome [Fig. 3(A)]. Fourth, it is likely that the scissile bond of (−)-EGCG is strained, suggesting lowering of the activation energy for the formation of the tetrahedral intermediate in the proposed acylation reaction (Fig. 4). Finally, it was observed that one of the two docked structures of lowest docked free energy for (−)-EGCG had its electrophilic carbonyl carbon 3.18 Å from the hydroxyl group of Thr 1 [Figs. 2(A) and (B)]. All these properties shown by this reported docking model have supplied an attractive, empirically directed, analog-supported model of proteasome inhibition by the green tea polyphenol (−)-EGCG.

Our immediate future studies will focus on rationally designing and synthesizing new EGCG analogs based on the docking information and examining their proteasome-inhibitory activities in vitro and in vivo. We also plan to perform docking studies with (−)-EGCG to both the β1- and β2-subunits of the yeast 20S proteasome. In preliminary studies (unpublished observations), we have found that (−)-EGCG can dock to the β1-subunit in a docking mode that is very similar to that described in this article for (−)-EGCG docked to the β5-subunit. Moreover, the docked free energy for (−)-EGCG docked to the β1-subunit is almost identical to the docked free energy observed for its docking to the β5-subunit. There were no docking modes found for (−)-EGCG docked to the β2-subunit in which the distance between the Thr-1 hydroxyl group and the ester carbonyl carbon atom was <4.0 Å. A few structures were observed in which (−)-EGCG was bound to the surface of the protein and the distances of Thr-1 hydroxyl and ester carbonyl carbon were very close to 4.0 Å. But (−)-EGCG was not actually docked to the catalytic site; therefore, nucleophilic attack of the carbonyl group by Thr1 could not occur in this conformation. These results are consistent with our experimental observations.[28] We also plan to further demonstrate acylation of the β5s Thr 1 by (−)-EGCG via X-ray diffraction studies. It is our hope that a better mechanistic understanding of proteasome inhibition by (−)-EGCG will allow for the rational design of more potent and stable, but less toxic, GTP analogs for cancer prevention.

ACKNOWLEDGMENT

We thank Mr. Layne Norton (Eckerd College) for his assistance with some of the docking studies reported herein.

REFERENCES

1. Goldberg AL. Functions of the proteasome: the lysis at the end of the tunnel. Science 1995;268:522–523.
2. Groll M, Ditzel L, Lowe J, Stock D, Bochtler M, Bartunik HD, Huber R. Structure of 20S proteasome from yeast at 2.4 A resolution. Nature 1997;386:463–471.
3. Seemuller E, Lupas A, Stock D, Lowe J, Huber R, Baumeister W. Proteasome from Thermoplasma acidophilum: a threonine protease. Science 1995;268:579–582.
4. Kisselev AF, Goldberg AL. Proteasome inhibitors: from research tools to drug candidates. Chem Biol 2001;8:739–758.
5. Dou QP, Nam S. Pharmacological proteasome inhibitors and their therapeutic potential. Exp Opin Ther Patents 2000;10:1263–1272.
6. Dou QP, Li B. Proteasome inhibitors as potential novel anticancer agents. Drug Resist Updat 1999;2:215–223.
7. Almond JB, Cohen GM. The proteasome: a novel target for cancer chemotherapy. Leukemia 2002;16:433–443.
8. An B, Goldfarb RH, Siman R, Dou QP. Novel dipeptidyl proteasome inhibitors overcome Bcl-2 protective function and selectively accumulate the cyclin-dependent kinase inhibitor p27 and induce apoptosis in transformed, but not normal, human fibroblasts. Cell Death Differ 1998;5:1062–1075.
9. Lopes UG, Erhardt P, Yao R, Cooper GM. p53-dependent induction of apoptosis by proteasome inhibitors. J Biol Chem 1997;272: 12893–12896.
10. Adams J, Palombella VJ, Sausville EA, Johnson J, Destree A, Lazarus DD, Maas J, Pien CS, Prakash S, Elliott PJ. Proteasome inhibitors: a novel class of potent and effective antitumor agents. Cancer Res 1999;59:2615–2622.
11. Sun J, Nam S, Lee CS, Li B, Coppola D, Hamilton AD, Dou QP, Sebti SM. CEP1612, a dipeptidyl proteasome inhibitor, induces p21WAF1 and p27KIP1 expression and apoptosis and inhibits the growth of the human lung adenocarcinoma A-549 in nude mice. Cancer Res 2001;61:1280–1284.
12. Adams J, Behnke M, Chen S, Cruickshank AA, Dick LR, Grenier L, Klunder JM, Ma YT, Plamondon L, Stein RL. Potent and selective inhibitors of the proteasome: dipeptidyl boronic acids. Bioorg Med Chem Lett 1998;8:333–338.
13. Adams J. Development of the proteasome inhibitor PS-341. Oncologist 2002;7:9–16.
14. Dou QP, Goldfarb RH. Evaluation of the proteasome inhibitor MLN-341 (PS-341). IDrugs 2002;5:828–834.
15. Groll M, Koguchi Y, Huber R, Kohno J. Crystal structure of the 20 S proteasome:TMC-95A complex: a non-covalent proteasome inhibitor. J Mol Biol 2001;311:543–548.
16. Ohno Y, Wakai K, Genka K, Ohmine K, Kawamura T, Tamakoshi A, Aoki R, Senda M, Hayashi Y, Nagao K, et al. Tea consumption and lung cancer risk: a case-control study in Okinawa, Japan. Jpn J Cancer Res 1995;86:1027–1034.
17. Zhong L, Goldberg MS, Gao YT, Hanley JA, Parent ME, Jin F. A population based case-control study of lung cancer and green tea consumption among women living in Shanghai, China. Epidemiology 2001;12:695–700.
18. Ji BT, Chow WH, Hsing AW, McLaughlin JK, Dai Q, Gao YT, Blot WJ, Fraumeni JF Jr. Green tea consumption and the risk of pancreatic and colorectal cancers. Int J Cancer 1997;70:255–258.
19. Inoue M, Tajima K, Mizutani M, Iwata H, Iwase T, Miura S, Hirose K, Hamajima N, Tominaga S. Regular consumption of green tea and the risk of breast cancer recurrence: follow-up study from the Hospital-based Epidemiologic Research Program at Aichi Cancer Center (HERPACC), Japan. Cancer Lett 2001;167:175–182.
20. Taniguchi S, Fujiki H, Kobayashi H, Go H, Miyado K, Sadano H, Shimokawa R. Effect of (−)-epigallocatechin gallate, the main constituent of green tea, on lung metastasis with mouse B16 melanoma cell lines. Cancer Lett 1992;65:51–54.
21. Wang ZY, Huang MT, Ho CT, Chang R, Ma W, Ferraro T, Reuhl KR, Yang CS, Conney AH. Inhibitory effect of green tea on the growth of established skin papillomas in mice. Cancer Res 1992;52: 6657–6665.
22. Liao S, Umekita Y, Guo J, Kokontis JM, Hiipakka RA. Growth inhibition and regression of human prostate and breast tumors in athymic mice by tea epigallocatechin gallate. Cancer Lett 1995;96: 239–243.
23. Gupta S, Ahmad N, Mohan RR, Husain MM, Mukhtar H. Prostate cancer chemoprevention by green tea: in vitro and in vivo inhibition of testosterone-mediated induction of ornithine decarboxylase. Cancer Res 1999;59:2115–2120.
24. Muto S, Yokoi T, Gondo Y, Katsuki M, Shioyama Y, Fujita K, Kamataki T. Inhibition of benzo[a]pyrene-induced mutagenesis by (−)-epigallocatechin gallate in the lung of rpsL transgenic mice. Carcinogenesis 1999;20:421–424.

25. Fujiki H. Two stages of cancer prevention with green tea. J Cancer Res Clin Oncol 1999;125:589–597.
26. Yang CS. Tea and health. Nutrition 1999;15:946–949.
27. Ahmad N, Mukhtar H. Green tea polyphenols and cancer: biologic mechanisms and practical implications. Nutr Rev 1999;57:78–83.
28. Nam S, Smith DM, Dou QP. Ester bond-containing tea polyphenols potently inhibit proteasome activity in vitro and in vivo. J Biol Chem 2001;276:13322–13330.
29. Smith DM, Wang Z, Kazi A, Li LH, Chan TH, Dou QP. Synthetic analogs of green tea polyphenols as proteasome inhibitors. Mol Med 2002;8:382–392.
30. Li L, Chan TH. Enantioselective synthesis of epigallocatechin-3-gallate (EGCG), the active polyphenol component from green tea. Org Lett 2001;3:739–741.
31. Berman HM, Westbrook J, Feng Z, Gilliland G, Bhat TN, Weissig H, Shindyalov IN, Bourne PE. The Protein Data Bank. Nucleic Acids Res 2000;28:235–242.
32. Morris GM, Goodsell DS, Halliday RS, R H, Hart WE, Belew RK, Olson AJ. Automated docking using a Lamarckian genetic algorithm and an empirical binding free energy function. J Comput Chem 1998;19:1639–1662.
33. Dym O, Xenarios I, Ke H, Colicelli J. Molecular docking of competitive phosphodiesterase inhibitors. Mol Pharmacol 2002;61:20–25.
34. Rao MS, Olson AJ. Modelling of factor Xa-inhibitor complexes: a computational flexible docking approach. Proteins 1999;34:173–183.
35. DeLano WL. The PyMOL Molecular Graphics System 2002. San Carlos, CA: DeLano Scientific; 2002.
36. Vicentini CB, Guarneri M, Andrisano V, Guccione S, Langer T, Marschhofer R, Chabin R, Edison AM, Huang X, Knight WB, Giori P. Potential of pyrazolooxadiazinone derivatives as serine protease inhibitors. J Enzyme Inhib 2001;16:15–34.
37. Dick LR, Cruikshank AA, Grenier L, Melandri FD, Nunes SL, Stein RL. Mechanistic studies on the inactivation of the proteasome by lactacystin: a central role for clasto-lactacystin beta-lactone. J Biol Chem 1996;271:7273–7276.
38. Antonov VK, Ivanina TV, Ivanova AG, Berezin IV, Levashov AV, Martinek K. Binding-catalysis relationship in alpha-chymotrypsin action as revealed from reversible inhibition study of phenylalkylboronic acids. FEBS Lett 1972;20:37–40.
39. da Graca Thrige D, Buur JR, Jorgensen FS. Substrate binding and catalytic mechanism in phospholipase C from Bacillus cereus: a molecular mechanics and molecular dynamics study. Biopolymers 1997;42:319–336.
40. Binda C, Angelini R, Federico R, Ascenzi P, Mattevi A. Structural bases for inhibitor binding and catalysis in polyamine oxidase. Biochemistry 2001;40:2766–2776.
41. Bravo L. Polyphenols: chemistry, dietary sources, metabolism, and nutritional significance. Nutr Rev 1998;56:317–333.